



Article

# Sound Absorption of the Water Column and Its Calibration for Multibeam Echosounder Backscattered Mapping in the East Sea of Korea

Seung-Uk Im <sup>1</sup>, Cheong-Ah Lee <sup>1</sup>, Moonsoo Lim <sup>2</sup>, Changsoo Kim <sup>3,\*</sup> and Dong-Guk Paeng <sup>1,\*</sup>

<sup>1</sup> Department of Ocean System Engineering, Jeju National University, Jeju-si 63243, Republic of Korea

<sup>2</sup> MarineResearch Co., Busan 49127, Republic of Korea

<sup>3</sup> Research Institute of Basic Science, Jeju National University, Jeju-si 63243, Republic of Korea

\* Correspondence: yustchangjnu@jejunu.ac.kr (C.K.); paeng@jejunu.ac.kr (D.-G.P.)

**Abstract:** Multibeam echosounder (MBES) backscatter data are influenced by underwater sound absorption, which is dependent on environmental parameters such as temperature, salinity, and depth. This study leverages CTD datasets from the Korea Oceanographic Data Center (KODC) to analyze and visualize the spatiotemporal variations in absorption parameters in the East Sea of Korea, which are subject to pronounced variability over time and space. The legacy MBES backscatter data, originally processed using generalized absorption parameters that neglected spatiotemporal variations, were compared with the calibrated data. The calibration process included inverse calculation of water temperature with depth-specific average salinity values from the nearest KODC stations. This calibration revealed discrepancies of up to 2.1 dB in backscatter intensity across survey lines, highlighting the potential misrepresentation of legacy MBES backscatter data due to site-specific absorption variability having been overlooked. By addressing these discrepancies, this study underscores the importance of incorporating spatiotemporal absorption variability into MBES calibration workflows. This integrated approach not only enhances the reliability of legacy MBES data but also provides valuable insights for marine resource management, seafloor mapping, and environmental monitoring in highly dynamic marine environments such as the East Sea of Korea.



Academic Editors: Ioannis Vakalas, Irene Zananiri and Henry Vallius

Received: 14 November 2024

Revised: 7 January 2025

Accepted: 14 January 2025

Published: 23 January 2025

**Citation:** Im, S.-U.; Lee, C.-A.; Lim, M.; Kim, C.; Paeng, D.-G. Sound

Absorption of the Water Column and Its Calibration for Multibeam Echosounder Backscattered Mapping in the East Sea of Korea. *Appl. Sci.* **2025**, *15*, 1131. <https://doi.org/10.3390/app15031131>

**Copyright:** © 2025 by the authors. Licensee MDPI, Basel, Switzerland. This article is an open access article distributed under the terms and conditions of the Creative Commons Attribution (CC BY) license (<https://creativecommons.org/licenses/by/4.0/>).

## 1. Introductions

Multibeam echosounder (MBES) backscatter data require careful consideration of environmental factors, particularly variations in water column properties such as temperature, salinity, and depth [1–4]. These variations significantly influence the propagation of sound in water, directly affecting bathymetric measurements and backscatter intensity data. Without accounting for these factors, the analysis of seabed characteristics may yield inconsistent results, especially in regions with dynamic oceanographic conditions [5–7].

MBES systems are widely used in marine research and industrial applications, including for seabed mapping, navigation surveys, marine resource exploration, and environmental monitoring. They provide bathymetric data reflecting the topography and morphology of the seabed, alongside backscatter intensity data indicating the acoustic signal strength from the seabed. Both data types are essential for analyzing the physical characteristics and spatial distribution of seabed substrates in marine environments [8–13].

Globally, MBES has become a cornerstone technology for detailed seabed characterization and habitat mapping [6,8]. However, traditional approaches to processing backscatter data often rely on empirical models or averaged water column values, which fail to account for site-specific or temporally varying oceanographic conditions. This has led to discrepancies in the interpretation of backscatter data, particularly in areas characterized by complex environmental variability [5,7,14–17].

The Korean seas present unique challenges for MBES data processing, due to their highly variable seasonal and regional environmental characteristics. Influenced by major currents such as the Kuroshio and Liman currents, these waters exhibit significant changes in temperature and salinity across different regions and seasons [18–22]. For example, localized shifts in salinity and temperature caused by these currents directly impact the speed of sound and absorption loss in seawater, resulting in variability in backscatter intensity. Despite these challenges, limited research has addressed the integration of site-specific water column parameters into MBES backscatter data processing approaches, particularly considering Korean waters [19,20,23,24].

In Korea, a significant portion of legacy MBES data were collected primarily for simple surveying purposes, rather than scientific research. As a result, these datasets were processed using empirical formulas or without consideration of water column properties at all, failing to reflect temporal and spatial variations in oceanographic conditions [25]. Such practices ignore the physical changes in the water column during data acquisition, leading to potential discrepancies in the backscatter intensity results. These discrepancies are particularly pronounced in regions, such as the Korean seas, with significant seasonal and regional environmental variability. This underscores the need for a systematic approach to re-process legacy MBES data using measured water column parameters [16,17].

This study aims to address these limitations by utilizing site-specific Sound Velocity Profiler (SVP) and Conductivity–Temperature–Depth (CTD) data to re-evaluate legacy MBES datasets. By correcting MBES datasets that have not adequately considered water column parameters, this study evaluates how underwater absorption affects MBES backscatter data. By re-calculating the absorption loss using water column information and integrating site-specific parameters such as temperature, salinity, and depth, the study seeks to mitigate discrepancies in the backscatter results. This approach enhances the representativeness of legacy MBES datasets in explaining the physical variability of the marine environment, thus improving their applicability for secondary analysis in scientific research and industrial applications. Furthermore, it highlights the importance of collecting water column information during MBES measurements, especially in dynamic environments such as the Korean seas [5–7,26,27].

## 2. Materials and Methods

### 2.1. Data Processing

Figure 1 shows the proposed workflow, investigating the impact of sound absorption of the water column while excluding other parameters, in order to better understand its contribution to backscatter variations.

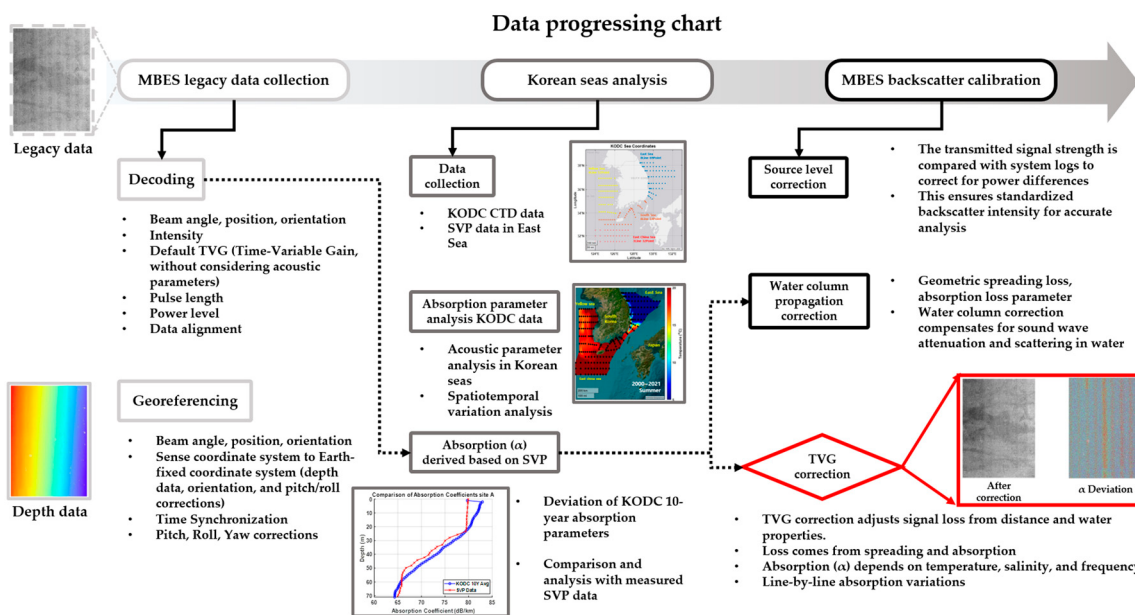


**Figure 1.** Workflow for calibrating legacy MBES data using historical KODC CTD and SVP data to improve backscatter measurements, including parameter explanations for each stage.

The legacy MBES data used in this study were collected from three coastal sites in the East Sea of Korea near survey Lines 102, 208, and 209, as depicted in Figure 2. Legacy MBES data acquisition was conducted using the Kongsberg EM3000 and EM2040C MBES systems (Kongsberg, Norway) installed aboard the Ocean 2000 vessel operated by the Korea Hydrographic and Oceanographic Agency. The raw MBES data were recorded using Kongsberg's Seafloor Information System software (SIS5, Kongsberg, Norway) [1,2]. The legacy MBES backscatter data, originally collected for non-research purposes, were obtained without adequately considering site-specific water column variability. However, the Korean seas exhibit significant temporal and spatial variability in oceanographic conditions due to dynamic factors such as seasonal currents and regional characteristics. To analyze the extent of these variations, historical CTD datasets from the Korea Oceanographic Data Center (KODC) were utilized to visualize and assess the spatiotemporal changes in absorption parameters across the East Sea. At locations where legacy MBES data were acquired, site-specific SVP measurements during the surveys were used and compared with the 10-year averaged KODC data to evaluate the deviations in absorption parameters. Using the mean salinity values derived from the KODC CTD data, water temperature profiles were estimated using the SVP measurements obtained from the legacy MBES surveys. These updated parameters were then applied to re-process the legacy MBES backscatter data.

The calibration workflow for legacy MBES datasets began with decoding of the raw MBES data to extract key acoustic parameters, including beam angle, position, orientation, pulse length, power level, and backscatter intensity [28]. In the decoding stage, Time-Variable Gain (TVG)—which was previously applied without considering site-specific acoustic conditions—was re-assessed to account for signal loss due to water column absorption.

Following the decoding phase, georeferencing was performed to align the MBES data with the Earth-fixed coordinates. This step involved correcting vessel motion parameters, such as pitch, roll, and heave, and synchronizing sensor data with precise positional information. The integration of these corrections ensured accurate mapping of the backscatter data to their corresponding seafloor locations.

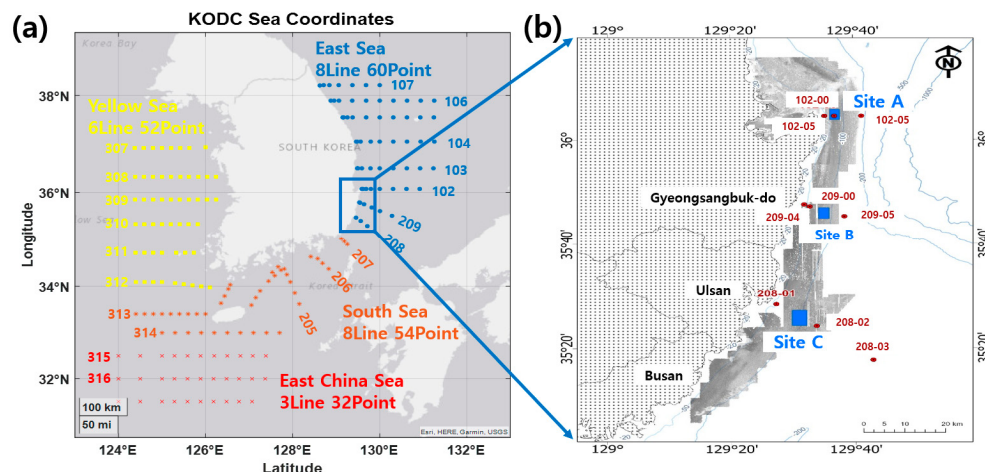


**Figure 2.** (a) Map of all survey lines and points in Korean territorial waters where CTD data were collected by KODC (KODC oceanographic survey map); and (b) three specific sites off the East Sea coast used for MBES measurements (Sites A, B, and C).

In the next phase, source level correction was applied. The transmitted signal strength was compared with system log values to correct for power variations during data acquisition. This step standardized the backscatter intensity measurements, making them suitable for comparative analysis across different regions and conditions.

The effects of sound absorption through the water column on the MBES backscatter data were investigated. Geometric spreading loss and absorption loss parameters were re-calculated using site-specific water column information derived from the KODC datasets. Absorption loss—represented by the absorption coefficient ( $\alpha$ )—was determined based on salinity, temperature, and frequency, enabling more precise compensation for signal attenuation and scattering effects.

The final step involved applying Time-Variable Gain (TVG) correction using the re-calculated absorption coefficients. This step mitigated the signal loss caused by distance and water column variability by performing line-by-line adjustments of the backscatter intensity data. By focusing specifically on the absorption parameter of the water column, this workflow isolated its contribution to backscatter variations while excluding other factors.

## 2.2. Sound Absorption Coefficient Analysis

In order to determine the sound absorption coefficient in the East Sea, we applied the Francois–Garrison model, which accounts for the contributions of boric acid, magnesium sulfate, and pure water to sound absorption [29,30]. The sound absorption coefficient  $\alpha(f)$  was calculated using the following equation based on KODC data, while the MBES calibration results were based on the measured SVP data.

The sound absorption coefficient,  $\alpha(f)$ , is calculated using the following equation:

$$\alpha(f) = \frac{A_1 P_1 f_1^2}{f_1^2 + f^2} + \frac{A_2 P_2 f_2^2}{f_1^2 + f^2} + A_3 P_3 f^2 \text{ [dB/km]}, \quad (1)$$

where  $A_1 = 0.106 \frac{P_1}{f_1}$ ,  $P_1 = \frac{8.86}{\exp(0.78pH)}$ , and  $f_1 = 2.8 \sqrt{\frac{S}{35}} \times 10^{4 - \frac{1245}{T}}$ .

The absorption due to magnesium sulfate,  $\alpha_{\text{magnesium sulfate}}$ , is given by

$$\alpha_{\text{magnesium sulfate}} = \frac{A_2 P_2 f_2 f^2}{f_1^2 + f^2},$$

where  $A_2 = 0.52 \times S$ ,  $P_2 = 1$ , and  $f_2 = 8.17 \times 10^{8 - \frac{1990}{T}}$ .

The absorption due to pure water,  $\alpha_{pure\ water}$ , is given by

$$\alpha_{pure\ water} = A_3 P_3 f^2,$$

$$\text{where } A_3 = 4.937 \times 10^{-4} - \frac{2.59 \times 10^{-5}}{T} + \frac{9.11 \times 10^{-7}}{T^2}.$$

To clearly identify the overall trend of sound absorption across different water layers in the East Sea, we calculated the total sound absorption. Total absorption in the East Sea was determined by integrating the absorption coefficient with respect to depth and adding it to the maximum depth, in order to account for the total absorption with respect to bidirectional propagation through the entire water column. The formula for total absorption (2) for a bidirectional path is

$$\sum_{n=0}^{MaxDepth} \alpha_{n+1} = 2\alpha_{Total} [\text{dB}]. \quad (2)$$

Finally, to analyze the overall sound absorption trend across the water column in the East Sea, we calculated the total absorption using a frequency of 300 kHz, which is commonly used in MBES systems. The calculated results were then compared and validated against historical MBES seafloor data.

### 2.3. Data Collection

The dataset for the East Sea comprises CTD measurements collected by survey vessels of the National Institute of Fisheries Science (NIFS) from 1991 to 2021 and stored in the KODC. Each region of the Korean seas is divided into specific lines and stations, where the East Sea is categorized into 8 lines and 60 stations. CTD measurements were conducted every two months, in order to reflect both seasonal and long-term changes [31].

Although data collection began in 1991, issues such as unclear station information and data discontinuities occurred in the 1990s. Additionally, as summarized in Table 1, external factors such as typhoons, vessel repairs, and logistical challenges occasionally rendered certain data unusable. To ensure consistency in analysis, this study focused on data collected between 2000 and 2021. The KODC dataset provides vertical profiles at 12 standard depth points (0, 10, 20, 30, 50, 75, 100, 125, 200, 250, 300, and 500 m).

**Table 1.** Missing CTD data for the East Sea during 2011–2021.

Day	Missing Point	Reason
Apr. 2011	102, 208, 209 All line	Equipment error
Feb. 2017	102–00 Point	Unobserved
Apr. 2018	209–00 Point	Unobserved
Dec. 2018	208–02 Point	Unobserved
Dec. 2019	102, 208 All line	Unobserved

To calculate sound absorption at each station, coefficients were interpolated for these standard depths in order to align with the specific depths of each survey station. This interpolation process was performed under the assumption that temperature and salinity remain constant below 500 m [20]. The interpolation was conducted using the Akima interpolation method, which ensures smooth and accurate results for environmental datasets [32,33]. When compared with raw CTD data at every 1 m interval, the interpolated results from the standard depths showed minimal differences, validating this interpolation data from the standard depths. These differences are presented in the Supplementary Materials (Figure S5), highlighting the consistency between the interpolated and raw datasets.

For seasonal analysis, one representative month from each season was selected to evaluate the spatiotemporal variations in absorption parameters. As shown in Figure 2b,

specific coastal areas with available MBES seafloor data were selected for further analysis. Three stations were chosen, based on the availability of existing MBES datasets: Site A on Line 102, Site B on Line 209, and Site C on Line 208. At these sites, the absorption parameters derived from KODC data were compared with the site-specific SVP measured during MBES surveys, in order to identify deviations and analyze the impacts of the spatiotemporal variability of the water column on backscatter intensity.

### 3. Results

#### 3.1. Seasonal Variations of Temperature, Salinity, and Sound Speed

Figure 3 shows the regional distribution of depth- and time-averaged temperature, salinity, and sound velocity in the East Sea during August from 2000 to 2021. These figures highlight the regional differences in temperature and salinity during August. Temperature is the key factor affecting the speed of sound and sound absorption characteristics. When the overall variations across the East Sea were observed, August showed the most significant deviations among the months. Notably, the deviation in temperature (Figure 3a) showed a maximum variation of up to  $3^{\circ}\text{C}$  in the southern coastal areas of the East Sea.

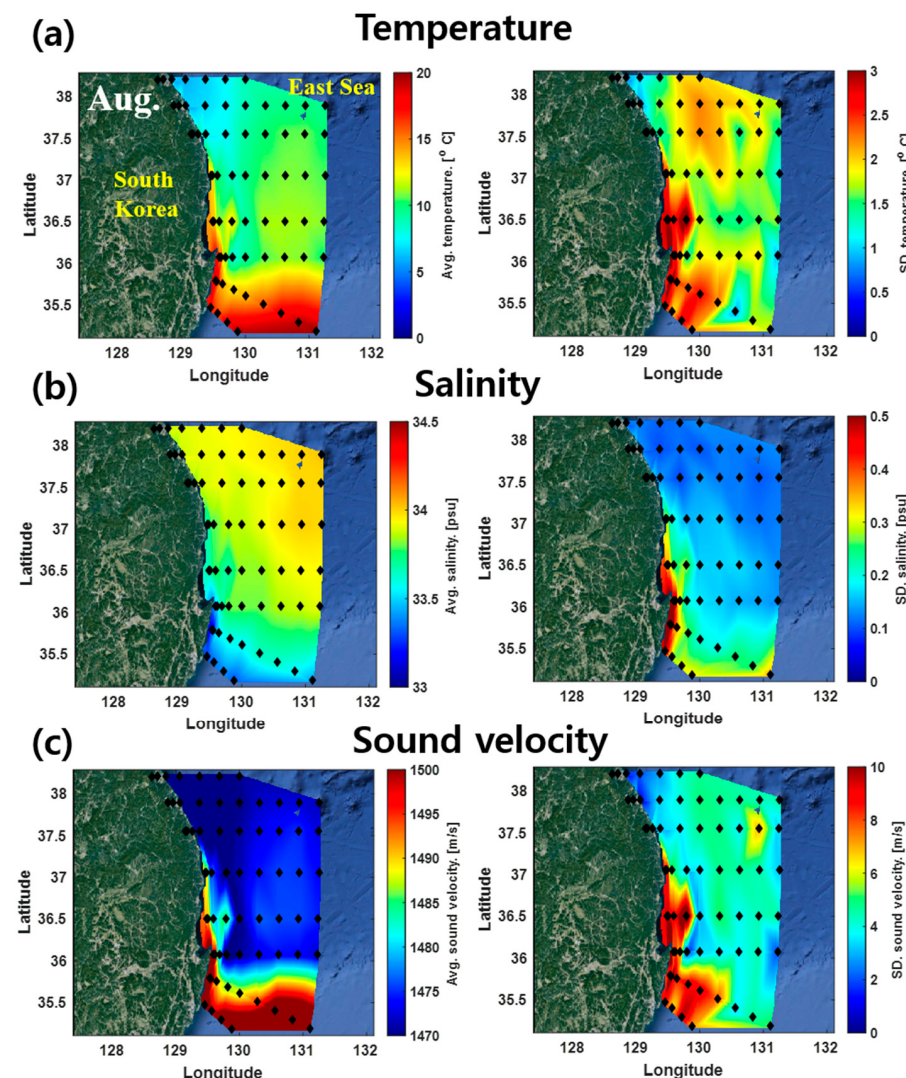


**Figure 3.** Distributions of depth- and time-averaged (a) temperature, (b) salinity, and (c) sound velocity and corresponding standard deviations in the East Sea of Korea for August from 2000 to 2021.

To further investigate the seasonal oceanographic changes in the East Sea, the mean and standard deviations of temperature (Figure S1), salinity (Figure S2), and sound velocity (Figure S3) are provided in the Supplementary Materials. During spring (April) and summer (August), surface water temperatures in some areas reached up to 25 °C, with salinity levels decreasing due to freshwater input and rainfall. In contrast, during fall (October) and winter (December), surface temperatures dropped as low as 2 °C, with salinity levels increasing due to reduced freshwater input and higher evaporation rates. The northern East Sea typically exhibited lower temperatures and higher salinity when compared with the southern part, leading to regional differences in sound velocity. These differences resulted in regional variations in sound velocity and acoustic properties.

Therefore, this study focused on identifying the differences in the southern coastal region of the East Sea, where the greatest variations in water temperature were observed, and in situ MBES surveys were performed. To simplify the process of obtaining results, a MATLAB (R2023a) GUI was implemented, as shown in Figure S4.

### 3.2. Total Underwater Sound Absorption

Figure 4a shows the total absorption for August averaged over 21 years from 2000 to 2021 in the East Sea. Total absorption was higher in the deeper regions, but the variation in the coastal area was also influenced by temperature and salinity. Figure 4b reveals a seasonal variation of the standard deviation of the total absorption at 15 coastal points (green stars marked in Figure 4a). The standard deviation of the total absorption coefficient was not affected by the depth. These results suggest that, even when measurements are taken in the same region during the same season, sound absorption coefficients can vary. Higher absorption deviation values generally occurred during summer (August) and winter (December), primarily due to greater fluctuations in water temperature. Conversely, lower deviation values of the total absorption were observed in spring (April) and fall (October).

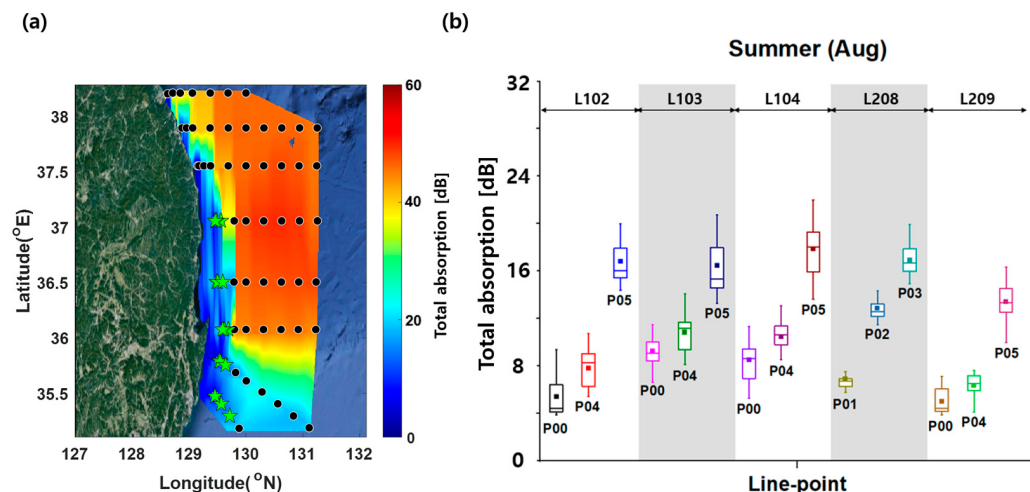


**Figure 4.** (a) The total absorption in August averaged from 2000 to 2021 in the East Sea. (b) Graphs showing standard deviation of total absorption at the 15 selected points in the southern coastal region of the East Sea during one month (August).

In particular, the 15 points with the most pronounced seasonal variations (green stars) showed lower total absorption due to shallower depths. However, similar to the variations in temperature, salinity, and sound velocity shown in Figure 3, higher changes in sound absorption were observed at these points. The region with the greatest deviation exhibited a difference of approximately 14 dB. These seasonal and regional variations highlight the importance of considering such fluctuations when calibrating MBES data, as they can significantly affect sound absorption.

To enhance the comprehension of the trends discerned in Figure 4b, the acoustic absorption fluctuations for seasons apart from summer are incorporated in Supplementary Figures S6–S8.

### 3.3. Sound Absorption from Water Temperature from SVP

The closest KODC measurement sites and the survey months corresponding to the MBES data collection were selected to conduct a comparative analysis between the historical temperature data from KODC and those inferred from the SVP measurements during MBES operations. The results, including temperature and absorption coefficient calculations, are shown in Figure 5.

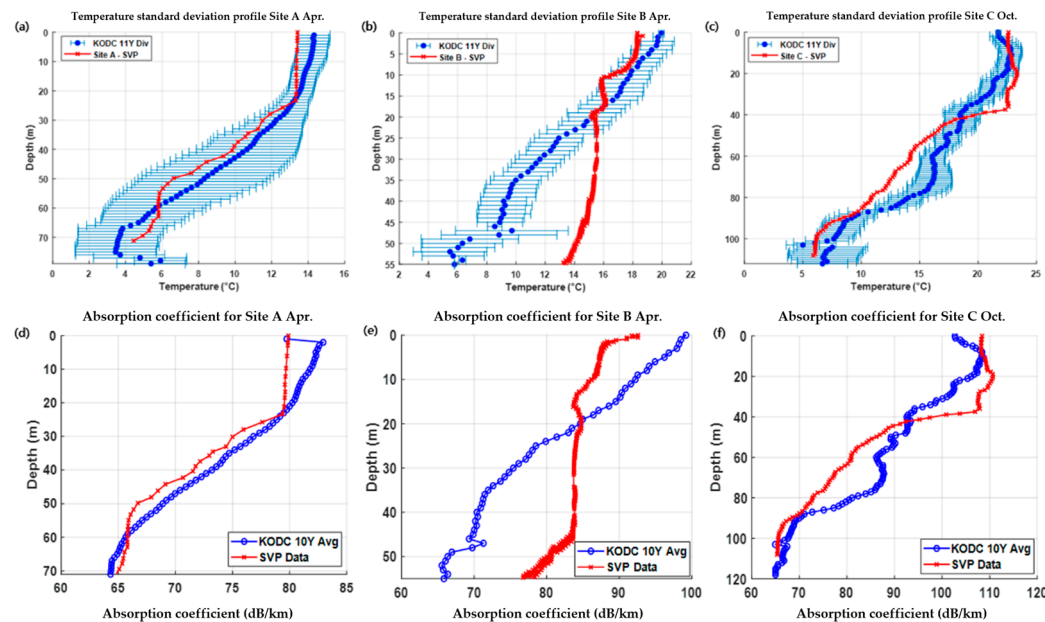


**Figure 5.** (a) Comparison of the 11-year mean and standard deviation of temperature at KODC 102-04 point (Site A) with SVP-derived water temperature in April. (b) Comparison of the 11-year mean and standard deviation of temperature at KODC 209-04 point (Site B) with SVP-derived water temperature in April. (c) Comparison of the 11-year mean and standard deviation of temperature at KODC 208-02 point (Site C) with SVP-derived water temperature in October. (d) Comparison of the absorption coefficients at Site A in April between the 11-year average KODC data and SVP data. (e) Comparison of the absorption coefficients at Site B in April between the 11-year average KODC data and SVP data. (f) Comparison of the absorption coefficients at Site C in October between the 11-year average KODC data and SVP data. The frequency was 300 kHz.

At Site A, the distance between the SVP measurement location and the KODC measurement point was approximately 180 m, with near-identical measurement times. The temperature derived from the SVP data was close to the 11-year (2010–2021) mean and within the standard deviation range of the KODC dataset. Temperature fluctuations ranged between 3.61 °C and 0.70 °C relative to the KODC mean. Similarly, the absorption coefficients calculated at Site A showed minimal deviation (<3 dB/km) from the KODC average, indicating high reliability in the corrections applied.

In contrast, Sites B and C exhibited significant spatial and temporal discrepancies. At Site B, the SVP measurement location was approximately 6 km away from the nearest KODC station, and the time difference between measurements was about 1 month. This resulted in notable differences in temperature (up to 8 °C) and absorption coefficients (up to 15 dB/km).

At Site C, the spatial separation was approximately 10 km, with a measurement time difference of more than 1 month. The temperature and absorption coefficient profiles showed substantial deviations, up to 5 °C and 15 dB/km, respectively.

SVP-based temperature and absorption coefficients at Site A were validated against the KODC dataset, thus confirming their reliability. However, for Sites B and C, the spatial and temporal differences led to inconsistencies in temperature and absorption coefficient values. These discrepancies underscore the importance of in situ measurements of SVP during MBES surveys.

This analysis highlights the importance of accounting for the spatiotemporal variability of temperature and absorption parameters when calibrating MBES backscatter data. Accurate water column measurements—particularly in dynamic environments such as the Korean seas—are essential for minimizing uncertainties in backscatter data and improving the reliability of re-calibrated results.

### 3.4. Multibeam Echosounder Calibration

The MBES maps collected from Site A (situated in proximity to the KODC 102 line-04 point) were processed employing the sound absorption coefficients obtained from SVP data. Historical oceanographic parameters recorded in April 2010, including a salinity measurement of 34 psu and temperature of 9 °C, served as the basis for data calibration. During the survey, the temperature from SVP indicated a marginally elevated temperature of 9.4 °C and salinity of 34.2 psu, culminating in a maximum discrepancy of 1.68 dB per line when computing the difference between the calibrated MBES backscattered intensity and the original uncalibrated outcomes. Figure 6 elucidates these differences, delineating the fluctuations in depth, original data, and the consequential effects of calibration of sound absorption on the backscattering map. The difference between the unprocessed and calibrated backscattered intensity was low but varied across the mapping lines.

Site B (located in proximity to the KODC 209 line-04 point) was subjected to a comparable data processing methodology, albeit with distinct variations in the environmental parameters. The map acquired from the MBES was initially calibrated using empirical measurements obtained in June 2019, which indicated a salinity level of 34.2 psu and a temperature of 9 °C. Nevertheless, the SVP recorded during the survey indicated a temperature of 10.6 °C, thereby necessitating modifications to the sound absorption coefficients. Following the application of these adjustments, the maximum deviation was reduced to 2.1 dB per line. Unlike Site A (Figure 6), Site B exhibited notable regional differences across the left, right, and central areas, highlighting variations in sound absorption across these sections. Figure 7 provides a comparative analysis of the depth profiles alongside the differences in sound absorption before and after the calibration process.

For Site C (located near the KODC 208 line-02 point), the MBES seafloor map was calibrated utilizing SVP measurements from September 2016. Due to the absence of concurrent CTD measurements, empirical data from October 2016—indicating a salinity of 33 psu and a back-calculated temperature of 16 °C—were employed. The actual SVP data during the survey revealed a salinity of 34 psu and a temperature of 15.62 °C, necessitating further calibration to align with these parameters. This calibration achieved a reduction in sound absorption discrepancies by 1.92 dB, as illustrated in Figure 8, which contrasts the raw and calibrated MBES maps. Site C represents the largest and most extensively mapped area, with less pronounced variations across individual lines but regional differences in the right central region (35° 26'). Site C exhibited larger discrepancies, although the differences were less extensive than those observed at Site B (Figure 7).

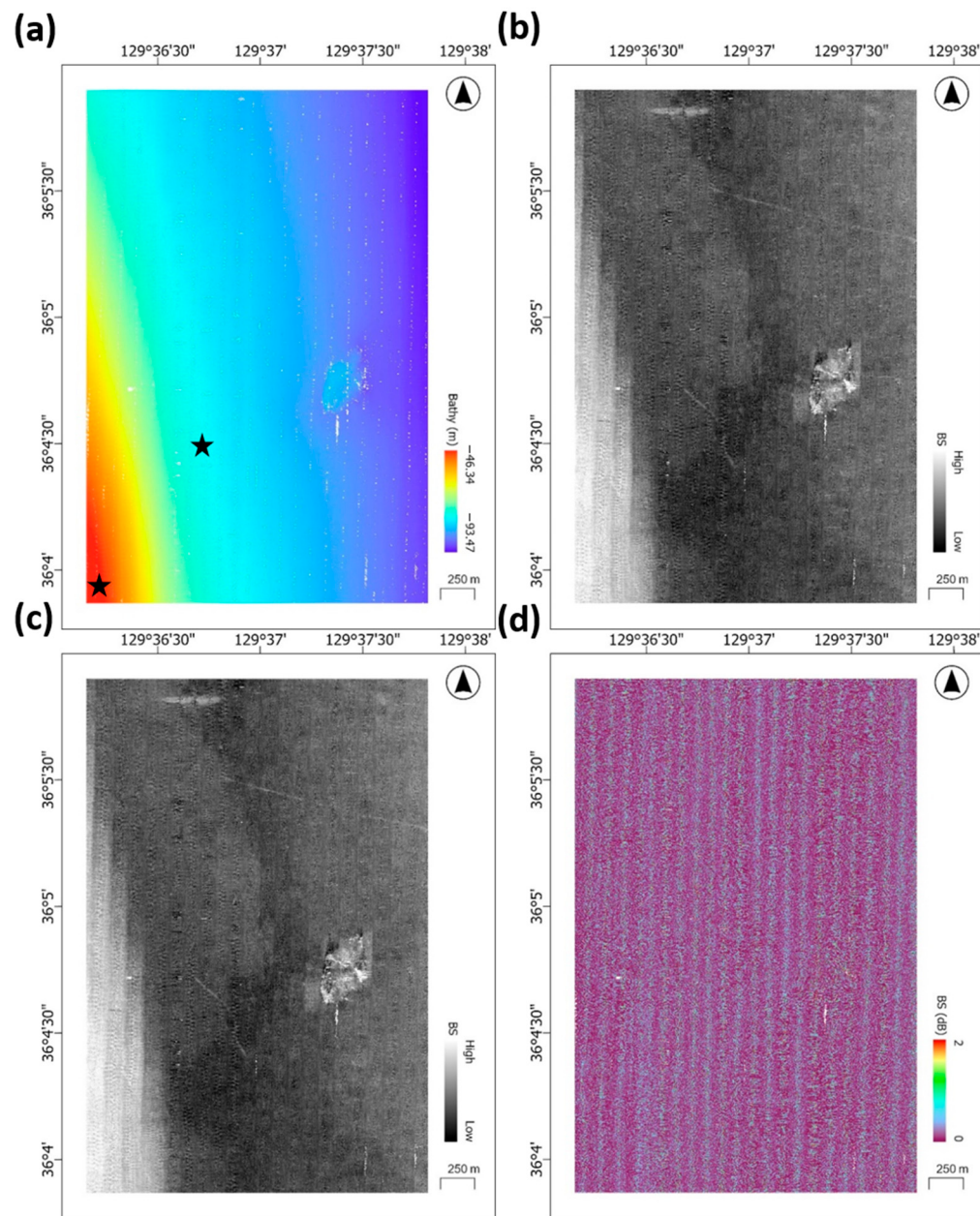


**Figure 6.** MBES maps and SVP-based calibration results at Site A: (a) Bathymetric map from MBES measurement with measurement points for water depth and SVP (black stars), (b) unprocessed legacy MBES backscattered map, (c) calibrated MBES backscattered map employing the sound absorption coefficient, and (d) differences between unprocessed legacy and calibrated backscattered values. Backscattering (BS) denotes the intensity of the backscattered signal (in dB) for the difference at each point.

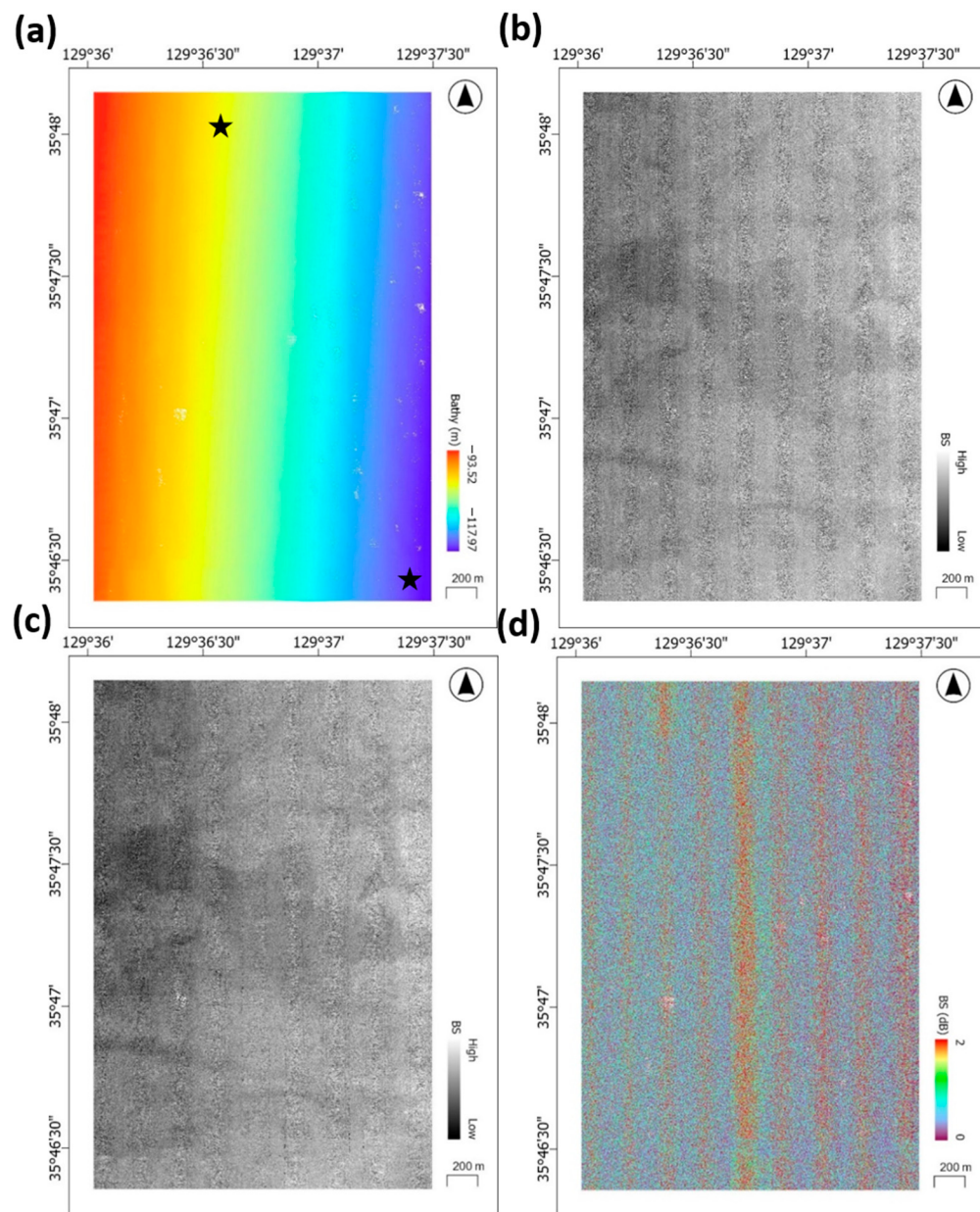


**Figure 7.** MBES data and SVP-based calibration results at Site B: (a) Bathymetric map from MBES measurement with measurement points for water depth and SVP (black stars), (b) unprocessed MBES backscattered map, (c) calibrated MBES backscattered map employing the sound absorption coefficient, and (d) differences between unprocessed and calibrated backscattered values. Backscattering (BS) denotes the intensity of the backscattered signal (in dB) for the difference at each point.

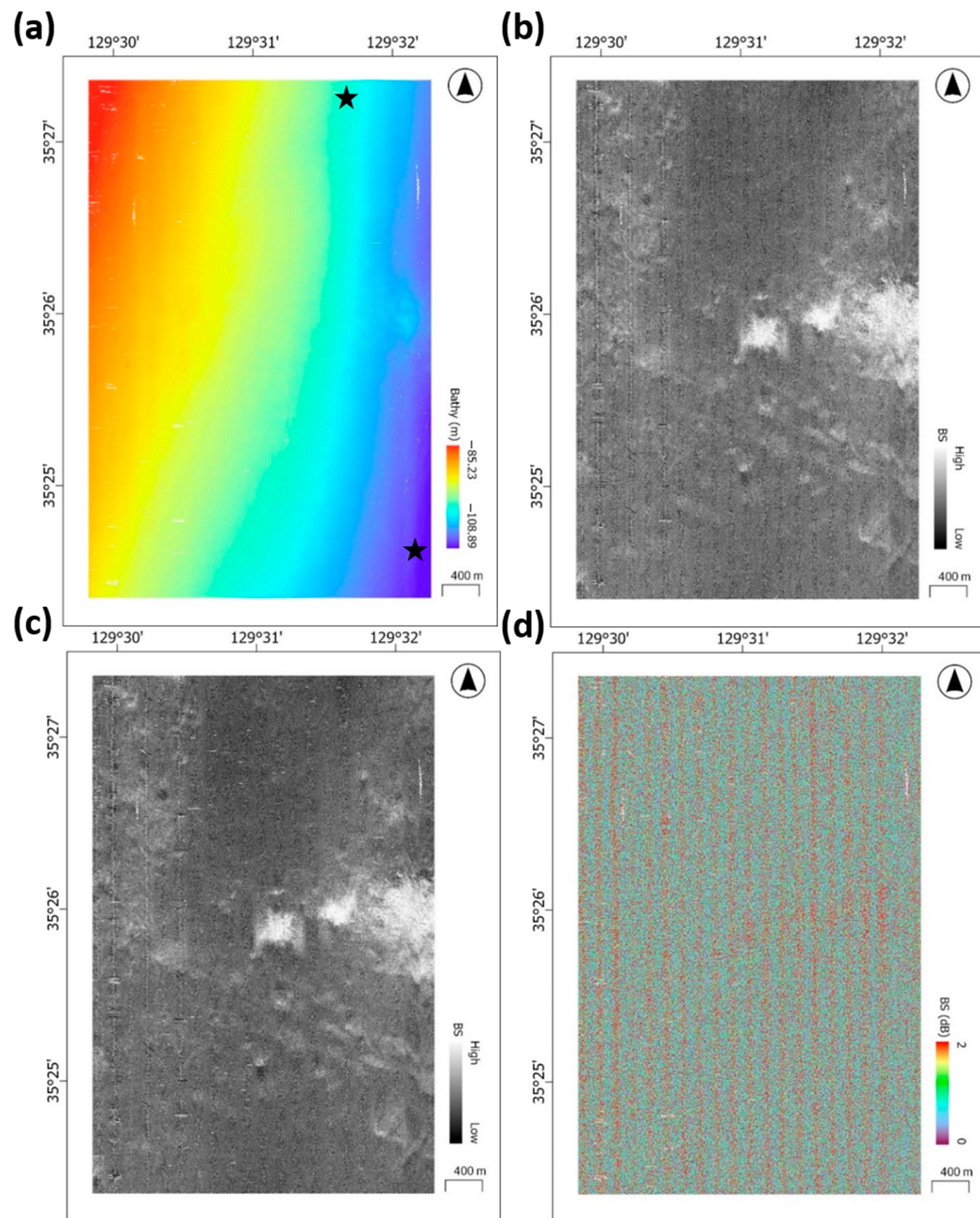


**Figure 8.** MBES data and SVP-based calibration results at Site C: (a) Bathymetric map from MBES measurement with measurement points for water depth and SVP (black stars), (b) unprocessed MBES backscattered map, (c) calibrated MBES backscattered map employing the sound absorption coefficient, and (d) differences between unprocessed and calibrated backscattered values. Backscattering (BS) denotes the intensity of the backscattered signal (in dB) for the difference at each point.

#### 4. Discussion

In this study, we evaluated the influence of sound absorption coefficients on MBES backscatter calibration in the East Sea of Korea. The results demonstrated that spatiotemporal variations in absorption coefficients arise due to seasonal and regional differences, driven by dynamic oceanographic processes such as cold currents and distinct water masses. By integrating site-specific parameters into the calibration workflow, we addressed these variations and improved the consistency of the calibrated backscatter data. Specifically, Site A—where the spatial and temporal discrepancies between SVP and historical KODC measurements were minimal—showed better agreement in the calibrated results. However, for

Sites B and C—where the spatial and temporal differences were more pronounced—greater discrepancies in backscatter intensity were observed [5–7].

The integration of SVP and historical CTD datasets enabled the calculation of sound absorption coefficients and re-processing of legacy MBES data. While historical CTD datasets provide a valuable resource for understanding long-term trends, they are constrained by physical limitations, such as the lengthy time required for data collection and processing. Similarly, SVP measurements also face certain physical limitations but offer more favorable conditions when compared with CTD datasets. SVP data are more practical for coastal surveys, due to their ease of acquisition and frequent availability, allowing for calibration of MBES datasets compared with the more resource-intensive CTD measurements. This distinction highlights the complementary role of SVP data in addressing some of the challenges associated with the sole use of CTD data in dynamic marine environments.

This study, while focusing on a specific case in the East Sea of Korea, provides valuable insights into the calibration of MBES backscatter data with the sound absorption of the water column in various oceanic environments. The differences in backscattered intensity between legacy MBES data and the data calibrated for the water column absorption, based on SVP and CTD data, may appear modest at up to 2.1 dB. However, these differences are significant when considered in the context of deeper waters operating at lower frequencies. Previous studies on absorption loss uncertainties have demonstrated that as operating frequencies decrease in deep oceans, particularly at 30 kHz, the impact of absorption loss becomes more pronounced [7]. For example, the maximum absorption loss uncertainty is 3.3 times greater in deep waters at 30 kHz compared with shallow waters at 300 kHz, illustrating a substantial amplification of uncertainty with greater depth and lower frequency. Expanding this methodology to other ocean environments with diverse oceanographic conditions would further validate its applicability and provide broader insights into MBES calibration practices.

Other studies have suggested frameworks for quantifying uncertainties in seafloor acoustic backscatter, which could serve as a reference for improving error estimates in calibration processes [29,30]. While this study primarily focused on evaluating spatiotemporal variations in sound absorption coefficients, we acknowledge the absence of a comprehensive sensitivity analysis as a limitation. Future work should include error budgets or uncertainty quantifications for the absorption parameters derived using models such as the Francois–Garrison formulation. Such analyses would strengthen the robustness of the calibrated MBES backscatter data, as well as providing additional insights into potential errors associated with environmental parameter estimation. When calculating absorption coefficients using SVP data, the calibrated backscatter data better reflected the local environmental conditions, reducing uncertainties associated with legacy datasets [1,25].

Despite the advantages of integrating SVP data, challenges remain under field conditions where neither SVP nor CTD measurements are readily available. In such cases, Expendable Bathymeters (XBTs) present a viable alternative for obtaining essential water column data. XBTs are cost-effective, portable, and capable of providing temperature profiles that can be combined with approximate salinity values from historical datasets to calculate sound absorption coefficients. While XBTs cannot directly measure salinity, this hybrid approach can mitigate the limitations of using historical data alone, providing a more robust framework for MBES calibration.

The observed deviations in absorption coefficients at Sites B and C underscore the limitations of relying solely on historical data, particularly when real-time SVP measurements are unavailable. However, legacy MBES datasets collected for non-research purposes can still be effectively re-processed if spatiotemporal conditions align with historical CTD or other reference datasets. This study highlights the need for operational guidelines during

MBES surveys, ensuring in situ water column measurements and their incorporation into the calibration process. Such protocols and guidelines can improve the consistency of MBES datasets and enhance their applicability in scientific research and industrial applications [5–7].

Future research should expand upon this study by investigating how other factors—including turbidity, suspended particles, and strong currents—fluence sound absorption and MBES backscatter intensity. Regions such as the South and West Seas, which are characterized by higher turbidity, dynamic currents, and increased suspended particle concentrations, present unique challenges. Understanding the contributions of these additional parameters can provide a more comprehensive approach for MBES calibration.

In summary, this study highlights the benefits of accounting for spatiotemporal variations in sound absorption coefficients when calibrating MBES backscatter data. By incorporating site-specific parameters into the calibration process, the consistency of legacy MBES datasets can be improved, thus contributing to more reliable seafloor mapping, effective marine resource management, and enhanced environmental monitoring in dynamic ocean environments such as the East Sea of Korea.

## 5. Conclusions

This study evaluated the impacts of absorption coefficients on MBES backscatter data calibration in the East Sea of Korea, integrating historical CTD datasets from the KODC and in situ SVP measurements. By calculating absorption coefficients and incorporating site-specific water column parameters, the calibration process reduced discrepancies in backscatter intensity, with differences of up to 2.1 dB observed. These results demonstrate the feasibility of re-processing legacy MBES datasets to better align with measured oceanographic conditions. The findings suggest the importance of understanding spatiotemporal variations in absorption parameters for MBES calibration. The influences of other environmental factors, such as turbidity and suspended particles, in regions such as the South and West Seas could be considered in future research, which may provide additional insights for the improvement of calibration methodologies.

**Supplementary Materials:** The following supporting information can be downloaded at <https://www.mdpi.com/article/10.3390/app15031131/s1>; Figure S1: Seasonal average and standard deviation of water temperature; Figure S2: Seasonal average and standard deviation of salinity; Figure S3: Seasonal average and standard deviation of sound velocity; Figure S4: Overview of the developed GUI; Figure S5: The interpolation of KODC data; Figure S5: Comparison between interpolated KODC standard depth data and 1 m interval raw measured; Figure S6. Standard deviation of total absorption at the 15 selected points in the southern coastal region of the East Sea season represented in April; Figure S7. Standard deviation of total absorption at the 15 selected points in the southern coastal region of the East Sea season represented in October; Figure S8. Standard deviation of total absorption at the 15 selected points in the southern coastal region of the East Sea season represented in December.

**Author Contributions:** Conceptualization, S.-U.I. and D.-G.P.; methodology, S.-U.I., C.K. and D.-G.P.; software, S.-U.I. and C.-A.L.; validation, S.-U.I., C.K. and D.-G.P.; formal analysis, S.-U.I.; investigation, S.-U.I.; resources, S.-U.I. and M.L.; data curation, S.-U.I.; writing—original draft preparation, S.-U.I.; writing—review and editing, S.-U.I., C.K. and D.-G.P.; visualization, S.-U.I.; supervision, D.-G.P.; project administration, C.K.; funding acquisition, D.-G.P. All authors have read and agreed to the published version of the manuscript.

**Funding:** This research was supported by the Korea Institute of Marine Science & Technology Promotion (KIMST) funded by the Ministry of Oceans and Fisheries (RS-2022-KS221578, RS-2023-00256122).

**Data Availability Statement:** Publicly available datasets were analyzed in this study. This data can be found in [https://www.nifs.go.kr/kodc/soo\\_list.kodc](https://www.nifs.go.kr/kodc/soo_list.kodc).

**Acknowledgments:** The authors thank Gee Soo Kong for their assistance in preparing the manuscript.

**Conflicts of Interest:** Author Moonsoo Lim was employed by the company MarineResearch Co. The remaining authors declare that the research was conducted in the absence of any commercial or financial relationships that could be construed as a potential conflict of interest.

## References

1. Schimel, A.C.; Beaudoin, J.; Parnum, I.M.; Le Bas, T.; Schmidt, V.; Keith, G.; Ierodiaconou, D. Multibeam sonar backscatter data processing. *Mar. Geophys. Res.* **2018**, *39*, 121–137. [[CrossRef](#)]
2. Lurton, X.; Lamarche, G.; Brown, C.; Lucieer, V.; RIce, G.; Schimel, A.; Weber, T. Backscatter measurements by seafloor-mapping sonars. In *Guidelines and Recommendations*; GeoHab: Brest, France, 2015; 200p.
3. Roh, J.; Choi, Y.; Yoon, H.; Lee, Y. Establishment error calibration method on MBES. *Spat. Inf. Res.* **2009**, *17*, 351–359.
4. Keyzer, L.; Mohammadloo, T.H.; Snellen, M.; Pietrzak, J.; Katsman, C.; Afrasteh, Y.; Guarneri, H.; Verlaan, M.; Klees, R.; Slobbe, C. Inversion of sound speed profiles from MBES measurements using Differential Evolution. *Proc. Meet. Acoust.* **2021**, *44*, 070035.
5. Malik, M. Estimation of Measurement Uncertainty of Seafloor Acoustic Backscatter. Doctoral Dissertation, University of New Hampshire, Durham, NH, USA, 2019.
6. Lucieer, V.; Roche, M.; Degrendele, K.; Malik, M.; Dolan, M.; Lamarche, G. User expectations for multibeam echo sounders backscatter strength data-looking back into the future. *Mar. Geophys. Res.* **2018**, *39*, 23–40. [[CrossRef](#)]
7. Malik, M.; Lurton, X.; Mayer, L. A framework to quantify uncertainties of seafloor backscatter from swath mapping echosounders. *Mar. Geophys. Res.* **2018**, *39*, 151–168. [[CrossRef](#)]
8. Brown, C.J.; Beaudoin, J.; Brissette, M.; Gazzola, V. Multispectral multibeam echo sounder backscatter as a tool for improved seafloor characterization. *Geosciences* **2019**, *9*, 126. [[CrossRef](#)]
9. Mohammadloo, T.H.; Snellen, M.; Simons, D.G. Assessing the performance of the multi-beam echo-sounder bathymetric uncertainty prediction model. *Appl. Sci.* **2020**, *10*, 4671. [[CrossRef](#)]
10. Cândido, R.M.A.M. Implementing a Reference Backscatter Calibration Technique on a Multi-Sector Multibeam Echosounder. Master’s Thesis, University of New Hampshire, Durham, NH, USA, 2022.
11. Gaida, T.C.; Tengku Ali, T.A.; Snellen, M.; Amiri-Simkoeei, A.; Van Dijk, T.A.; Simons, D.G. A multispectral Bayesian classification method for increased acoustic discrimination of seabed sediments using multi-frequency multibeam backscatter data. *Geosciences* **2018**, *8*, 455. [[CrossRef](#)]
12. Kruss, A.; Rucinska, M.; Grzadziel, A.; Waz, M.; Pocwiardowski, P. Multi-band, calibrated backscatter from high frequency multibeam systems as an efficient tool for seabed monitoring. In Proceedings of the 2023 IEEE Underwater Technology (UT), Tokyo, Japan, 6–9 March 2023; pp. 1–5.
13. Leroy, C.C.; Robinson, S.P.; Goldsmith, M.J. A new equation for the accurate calculation of sound speed in all oceans. *J. Acoust. Soc. Am.* **2008**, *124*, 2774–2782. [[CrossRef](#)]
14. Eleftherakis, D.; Berger, L.; Le Bouffant, N.; Pacault, A.; Augustin, J.; Lurton, X. Backscatter calibration of high-frequency multibeam echosounder using a reference single-beam system, on natural seafloor. *Mar. Geophys. Res.* **2018**, *39*, 55–73. [[CrossRef](#)]
15. Foote, K.G.; Chu, D.; Hammar, T.R.; Baldwin, K.C.; Mayer, L.A.; Hufnagle, L.C., Jr.; Jech, J.M. Protocols for calibrating multibeam sonar. *J. Acoust. Soc. Am.* **2005**, *117*, 2013–2027. [[CrossRef](#)] [[PubMed](#)]
16. Grzadziel, A. The importance of under-keel sound velocity sensor in measuring water depth with multibeam echosounder. *Energies* **2021**, *14*, 5267. [[CrossRef](#)]
17. Zhang, J.; Zhang, L.; Zhang, A.; Zhang, L.; Li, D.; Zhang, X. Improving the Estimation of Temperature and Salinity by Assimilation of Observed Sound Speed Profiles. *J. Atmos. Ocean. Technol.* **2021**, *38*, 1277–1289. [[CrossRef](#)]
18. Bok, T.; Kim, J.; Lee, C.; Bae, J.; Paeng, D.; Pang, I.; Lee, J. Performance of Underwater Communication in Low Salinity Layer at the Western Sea of Jeju. *J. Inst. Electron. Eng. Korea TC* **2011**, *48*, 16–24.
19. Lee, Y.; Park, M.; Kim, S. Spatiotemporal variations of marine environmental characteristics in the Middle East Coast of Korea in 2013–2014. *J. Korean Soc. Mar. Environ. Energy* **2016**, *19*, 274–285. [[CrossRef](#)]
20. Park, M.-O.; Lee, Y.-W.; Ahn, J.-B.; Kim, S.-S.; Lee, S.-M. Spatiotemporal distribution characteristics of temperature and salinity in the coastal area of Korea in 2015. *J. Korean Soc. Mar. Environ. Energy* **2017**, *20*, 226–239. [[CrossRef](#)]
21. Kim, H.; Yamaguchi, H.; Yoo, S.; Zhu, J.; Okamura, K.; Kiyomoto, Y.; Tanaka, K.; Kim, S.; Park, T.; Oh, I.S. Distribution of Changjiang diluted water detected by satellite chlorophyll-a and its interannual variation during 1998–2007. *J. Oceanogr.* **2009**, *65*, 129–135. [[CrossRef](#)]
22. Jun-Cheol, K.O.; Hong-Kil, R. Fluctuation characteristic of temperature and salinity in coastal waters around Jeju Island. *Korean J. Fish. Aquat. Sci.* **2003**, *36*, 306–316.

23. Kim, H.; Kim, J.; Paeng, D. Analysis of surface sound channel by low salinity water and its mid-frequency acoustic characteristics in the East China Sea and the Gulf of Guinea. *J. Acoust. Soc. Korea* **2015**, *34*, 1–11. [[CrossRef](#)]
24. Kim, K.; Kim, K.; Kim, Y.; Cho, Y.; Kang, D.; Takematsu, M.; Volkov, Y. Water masses and decadal variability in the East Sea (Sea of Japan). *Prog. Oceanogr.* **2004**, *61*, 157–174. [[CrossRef](#)]
25. Lim, M.; Jeong, J.B.; Yi, B.; Park, Y.; Hwang, S.; Kang, J. Enhancing Backscatter Data Processing Through Sound Speed and Salinity Proxies. *Ocean Sci. J.* **2024**, *59*, 63. [[CrossRef](#)]
26. Kim, J.; Kim, H.; Paeng, D. Analysis of haline channel formed in the East China Sea and the Atlantic Ocean using the TS gradient diagram. *J. Adv. Mar. Eng. Technol.* **2014**, *38*, 208–216. [[CrossRef](#)]
27. Hong-Kil, R. A study on China coastal water appeared in the neighbouring seas of Cheju Island. *Korean J. Fish. Aquat. Sci.* **1994**, *27*, 515–528.
28. Yang, F.; Li, J.; Han, L.; Liu, Z. The filtering and compressing of outer beams to multibeam bathymetric data. *Mar. Geophys. Res.* **2013**, *34*, 17–24. [[CrossRef](#)]
29. Francois, R.E.; Garrison, G.R. Sound absorption based on ocean measurements: Part I: Pure water and magnesium sulfate contributions. *J. Acoust. Soc. Am.* **1982**, *72*, 896–907. [[CrossRef](#)]
30. Francois, R.E.; Garrison, G.R. Sound absorption based on ocean measurements. Part II: Boric acid contribution and equation for total absorption. *J. Acoust. Soc. Am.* **1982**, *72*, 1879–1890. [[CrossRef](#)]
31. Kim, S.; Kim, H. Long-Term Spatiotemporal Oceanographic Data from the Northeast Pacific Ocean: 1980–2022 Reconstruction Based on the Korea Oceanographic Data Center (KODC) Dataset. *Data* **2023**, *8*, 175. [[CrossRef](#)]
32. Akima, H. A new method of interpolation and smooth curve fitting based on local procedures. *J. ACM (JACM)* **1970**, *17*, 589–602. [[CrossRef](#)]
33. Akima, H. A method of bivariate interpolation and smooth surface fitting based on local procedures. *Commun. ACM* **1974**, *17*, 18–20. [[CrossRef](#)]

**Disclaimer/Publisher's Note:** The statements, opinions and data contained in all publications are solely those of the individual author(s) and contributor(s) and not of MDPI and/or the editor(s). MDPI and/or the editor(s) disclaim responsibility for any injury to people or property resulting from any ideas, methods, instructions or products referred to in the content.